

Photodissociation of methanol at 193.3 nm: Translational energy release spectra

Y. Wen,^{a)} J. Segall,^{b)} M. Dulligan, and C. Wittig

Department of Chemistry, University of Southern California, Los Angeles, California 90089-0482

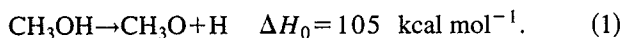
(Received 19 April 1994; accepted 14 June 1994)

Center-of-mass translational energy distributions of the dominant primary products resulting from 193.3 nm excitation of jet-cooled CH₃OH, CH₃OD, and CD₃OH were obtained by using the high-*n* Rydberg time-of-flight (HRTOF) technique. The appearance threshold in the HRTOF spectrum yields a bond dissociation energy, $D_0(\text{CH}_3\text{O}-\text{H})$, of $105 \pm 1 \text{ kcal mol}^{-1}$, in agreement with recent literature values. Translational energy release spectra from the three isotopomers exhibit progressions of $950 \pm 100 \text{ cm}^{-1}$, which are attributed to excitation in the ν_3 O-CH₃ stretch of the methoxy product. The progressions peak at $v = 1$, with population out to at least $v = 5$. This differs from the results of a recent wave packet dynamics study on a calculated excited state potential energy surface [Marston *et al.*, *J. Chem. Phys.* **98**, 4718 (1993)], which predicted no O-CH₃ stretch excitation in the methoxy fragment following photolysis of ground state methanol. The spatial anisotropy of the fragments ($\beta \sim -0.7$) implies a dissociation time ≤ 1 ps. The impulsive model for rotational excitation is compared to the unresolved rotational contour of the vibrational peaks in the translational energy release spectra and is found to underestimate the extent of rotational excitation, though the model correctly predicts the increase in contour width observed for the O-deuterated species. The unresolved rotational contours are fit empirically. The inferred vibrational energy distributions are discussed in terms of a simple Franck-Condon model for the pseudotriatomic, Me-O-H. Implications of the vibrational and rotational photofragment distributions for the full $1^1A''$ surface are discussed.

INTRODUCTION

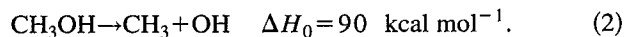
The photochemistry of gaseous methanol, at both infrared and ultraviolet wavelengths, has received considerable attention. This is due in part to the practical significance of methanol, which ranks tenth in U.S. production of organic chemicals, with 3.8×10^9 kg produced in 1992.¹ In addition, the relatively small number of electrons in methanol makes it amenable to high-level computational studies. In infrared multiple photon dissociation (IRMPD) studies,² it was found that, regardless of excitation frequency, the dominant primary products were the same as those seen in thermal excitation, namely, CH₃+OH.³ This is not surprising, since after the molecule has absorbed a number of infrared photons, further photoexcitation results in nonselective vibrational "heating" of the molecule within its ground electronic state until the lowest energy dissociation channel opens.

However, it is well established from end-product analyses,³⁻⁷ as well as the more recent nascent hydrogen atom detection study by Satyapal *et al.*,⁸ that the ultraviolet photolysis of methanol in its first absorption band ($S_1 \leftarrow S_0$) between 165 and 200 nm yields CH₃O+H as the dominant channel



Satyapal *et al.*⁸ estimated that reaction (1) accounts for $86\% \pm 10\%$ of the products at a photolysis wavelength of 193.3 nm, in agreement with the relative yield of this channel as determined by end-product analysis of methanol photolyzed

with the 184.9 nm line of a Hg lamp.^{3,4} Reaction (1) is significantly more endothermic than the dominant thermal process



All primary products thought to be involved in the S_1 photochemistry of methanol are listed in Table I along with their respective reaction endothermicities. We note that the accurate determination of the bond dissociation energy, $D_0(\text{CH}_3\text{O}-\text{H})$, or equivalently the methoxy heat of formation, has been the subject of extensive investigation.¹⁵ This value is important because of the central role methoxy plays in combustion and atmospheric chemistry.¹⁵

In addition to estimating the relative yield of the CH₃O+H channel, Satyapal *et al.* also reported that 82% of the available energy appeared as product translation from interpretation of Doppler line shapes of nascent H atoms.⁸ From the high translational energy release and the dominance of a thermodynamically disfavored process, it was concluded that the first absorption band of methanol accesses a potential energy surface (PES) that is repulsive in the O-H coordinate.⁸

Prior to the study by Satyapal *et al.*, several spectroscopic investigations assigned the broad, featureless first absorption band in simple alkyl alcohols to an $n-\sigma^*$ transition in which a lone pair electron on the oxygen is excited into an antibonding orbital oriented in the plane defined by the carbon, oxygen, and hydroxy hydrogen.¹⁶⁻¹⁸ While this assignment is consistent with the small or absent C-H cleavage channel, it does not provide a rationale for the observed propensity for O-H bond scission over C-O bond scission. Moreover, other spectroscopic studies have assigned this ab-

^{a)}Chemistry Department, University of Wisconsin, Madison, WI 53706.

^{b)}Chemistry Department, University of California, Irvine, CA 92717-2025.

TABLE I. Summary of enthalpy of reaction data for possible primary methanol photodecomposition channels.

Reaction products	$\Delta H_0(\text{kcal mol}^{-1})^a$	References
$\text{CH}_2\text{O}+2\text{H}$	123.6	9
$\text{CH}_3\text{O}+\text{H}$	105	10–12
$\text{CH}_2\text{OH}+\text{H}$	95	11–13
CH_3+OH	90	14
$\text{CH}_2\text{O}+\text{H}_2$	20.3	9

^aEstimated uncertainties are $\pm 2 \text{ kcal mol}^{-1}$.

sorption band as a $n-3s$ Rydberg transition,¹⁹ as have several theoretical investigations discussed below. One might naively expect a surface accessed by a Rydberg transition to have a local minimum near the ground state geometry for methanol. This is consistent with some of the earlier studies. For example, Hagège *et al.*⁵ reported that the uv photodissociation of methanol was collisionally activated at pressures of 10–100 Torr.⁵ On the other hand, Herasymowych and Knight⁶ reported collisional *deactivation* of photoexcited methanol in the same pressure range. Though contradictory, both of these results were interpreted as evidence of a long-lived excited state. However, this conclusion was refuted by Satyapal *et al.*⁸ who reported that the dominant process proceeds on a timescale of molecular rotation or faster.

Experimental evidence concerning the nature of the minor uv photolysis channels, which account for an estimated $14\% \pm 10\%$ of the photoproducts, remains somewhat contradictory. End product analyses indicate that CH_3+OH contributes only slightly to the overall yield,^{3–5} but investigators disagree on whether most of the remaining photochemical decomposition is through the C–H cleavage channel^{3,5} yielding $\text{CH}_2\text{OH}+\text{H}$ or the $\text{CH}_2\text{O}+\text{H}_2$ molecular elimination channel.^{4,7} Moreover, it should be noted that Satyapal *et al.*⁸ reported evidence for appreciable CH_3 formation. No direct detection of minor products from the uv photodissociation of methanol has been reported.

The experimental work on methanol photochemistry has been complemented by several theoretical studies.^{7,11,12,20–23} There is agreement that irradiation in the first absorption band excites methanol into the $3s$ Rydberg level,^{20,21} and that the corresponding $1^1A''$ hypersurface is purely repulsive along the O–H coordinate, with no minima from the valence region to products.^{21–23} Moreover, there is no inconsistency between Rydberg excitation and repulsion along the O–H coordinate because the $3s$ Rydberg character in the valence region correlates with σ^* character in the product channel through a process termed deRydbergization.^{7,21,22} In addition, there is consensus that the $1^1A''$ surface does not correlate to ground state $\text{CH}_2\text{OH}+\text{H}$ products,^{7,21,22} and therefore this channel is thought to be unimportant.⁷ A similar situation occurs for the molecular elimination channel that yields $\text{CH}_2\text{O}+\text{H}_2$, in that the $1^1A''$ surface correlates to excited formaldehyde,^{21,22} though a dissociation path with a relatively small barrier was calculated by Buenker *et al.*⁷

Though all calculations show that the $1^1A''$ surface correlates with ground state CH_3+OH , there is less agreement on whether there is a barrier for this process.^{7,21,23} The most recent calculation of this surface by Marston *et al.*²³ found

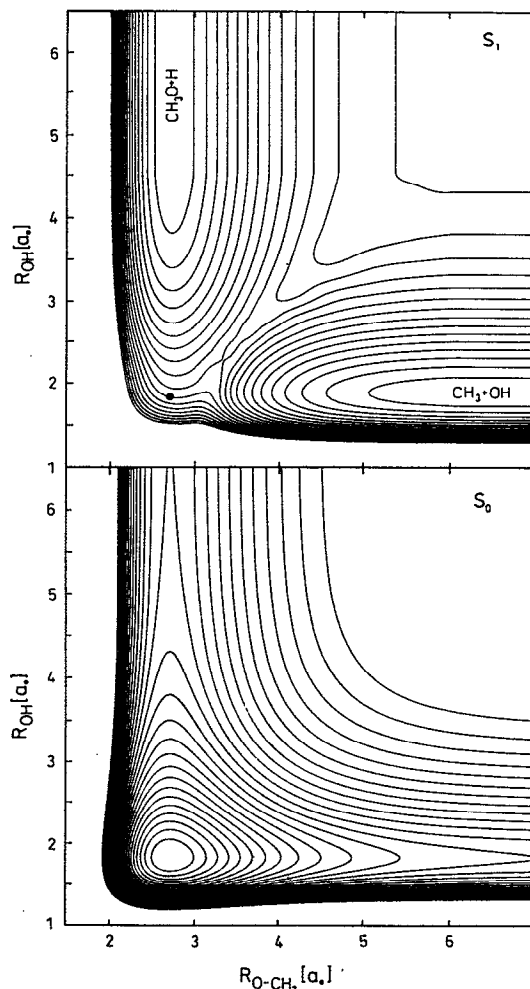


FIG. 1. The calculated ground (lower) and first excited (upper) PES's for methanol, taken from Marston *et al.* (Ref. 22). Contours correspond to 0.01 Hartree. The black dot on the upper PES indicates the Franck–Condon point.

that though both the C–O and O–H coordinates are repulsive, the Franck–Condon region lies on the $\text{CH}_3\text{O}+\text{H}$ side of the saddle point separating the two product valleys, as shown in Fig. 1. Following vertical excitation, methanol molecules near the equilibrium geometry for the ground electronic state therefore face a barrier to C–O bond scission while encountering no barrier to O–H bond breaking. Indeed, wave packet calculations on this surface indicate that excitation from the vibronic ground state leads exclusively to formation of $\text{CH}_3\text{O}+\text{H}$, while significant production of CH_3+OH requires at least 5 quanta of C–O stretch to overcome the barrier in the C–O coordinate.²³ As noted above, experimental evidence on the role of the CH_3+OH channel is somewhat equivocal.

Furthermore, the wave packet dynamics calculations of Marston *et al.* indicate that the dissociation of methanol via the first excited PES “proceeds in a vibrationally adiabatic way.”²³ In other words, $S_1 \leftarrow S_0$ excitation of methanol from its vibronic ground state should lead to formation of the vibrational ground state of methoxy, while excitation of metha-

nol having one quanta of HO-CH₃ stretch should yield a methoxy radical with one quanta of O-CH₃ stretch, and so forth. To test this prediction, we measured the translational energy release of H atoms from the photodissociation of jet-cooled methanol in its first absorption band, utilizing the high-*n* Rydberg time-of-flight (HRTOF) technique. We note that translational energy spectra, if obtained with sufficient resolution, carry useful information about the PES upon which the dissociation proceeds, and therefore experimental results can provide benchmarks for comparisons with theory.

EXPERIMENT

Our present experimental implementation of the HRTOF technique, which was pioneered by Welge and co-workers^{24,25} has been described previously.²⁶⁻²⁸ Briefly, a molecular beam containing the sample was photolyzed with the output from a 193 nm ArF excimer laser (Questek 2820), which was focused by a 1 m, lens and collimated by an iris before entering the vacuum chamber. Polarization was achieved by using eight quartz plates placed in the path of the ArF beam at Brewster's angle. Radiation from a XeCl excimer laser (Lambda Physik EMG 201 MSC) was split equally to pump two dye lasers. The 364.70 nm radiation from one dye laser (Lambda Physik 3002) was focused into a Kr cell to produce 121.57 nm Lyman- α radiation via frequency tripling.²⁹ The 121.57 nm radiation is focused into the interaction region by a MgF₂ lens. H and D atoms were excited by tuning the vuv radiation to the Lyman- α transitions for H and D atoms, which are separated by 21.4 cm⁻¹. To reduce ionization caused by residual 364.70 nm radiation, the combination of lenses was arranged in such a way that the 121.57 nm radiation was focused in the interaction region, while the 364.70 nm fundamental was defocused. Detection and alignment of the vuv radiation were accomplished by using a photoionization cell with an adjustable entrance iris and xyz positioner. This cell was connected to the reaction chamber with flexible bellows. The vuv radiation was estimated to have 10⁸ photons/pulse.

The output from the second probe laser (Lambda Physik 2001), which counterpropagates with the vuv radiation, further excites the hydrogen electron from the 2*p* orbital to a high-*n* Rydberg orbital. These high lying Rydberg states are optically metastable and thus drift with their nascent velocities until they pass through a wire mesh into a region with a moderate electric field (~1800 V/cm). The excited H atoms are rapidly and efficiently field ionized, then counted. The detector in these experiments was a Chevron MCP (Galileo Electro-Optics). The reception angle of the detector was 10⁻⁴ steradians with respect to the laser interaction region, while the TOF distance was 33.9 cm for all except some of the relative H/D studies, where it was 24 cm. Ion signals were amplified (Comlinear, CLC102), digitized by a transient digitizer (DSP, Transiac 2001) and processed in a computer. The experimental resolution for this work was ~170 cm⁻¹ at 20 000 cm⁻¹, which was determined from the FWHM of the peaks in HRTOF spectrum from 193 nm HBr photolysis.

A 3% CH₃OH/He mixture was obtained by bubbling He through methanol at a total pressure of 400 Torr. The low stagnation pressure was chosen to avoid formation of weakly

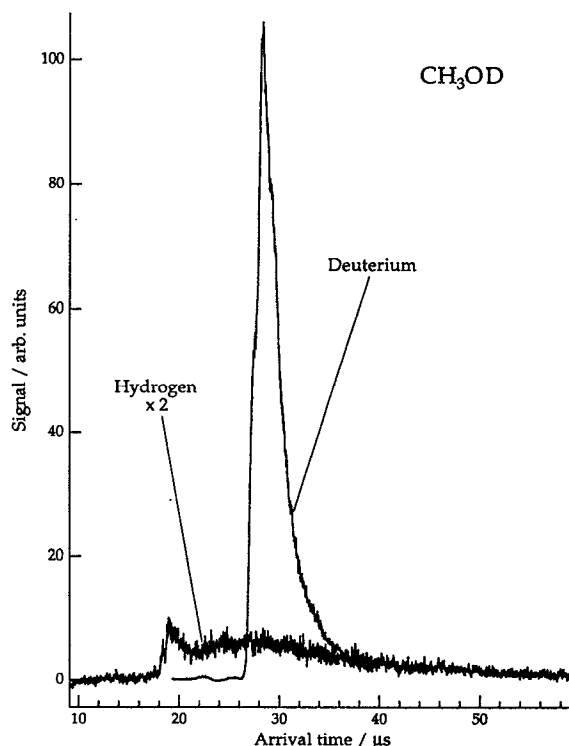


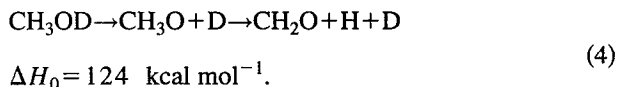
FIG. 2. Hydrogen and deuterium atom TOF spectra from photolysis of CH₃OD, with a flight path of 33.9 cm.

bound complexes, which are known to affect translational energy release spectra.^{27,28} This mixture was expanded into the source chamber through a 500 μ m diameter pulsed nozzle (General Valve), operating at a repetition rate of 10 Hz with a pulse width of 500 μ s. The molecular beam was collimated by a 1 mm diameter skimmer located 2 cm from the orifice; the laser beams crossed the molecular beam at a point 5 cm downstream from the skimmer. The molecular beam was monitored by a quadrupole mass spectrometer (UTI100C). CH₃OH, CH₃OD, and CD₃OH (Aldrich) were used without purification. For deuterated samples, the manufacturer specifies an isotopic purity of 99.5+ percent.

RESULTS AND DISCUSSION

TOF spectra of nascent H and D atom photofragments obtained from photolysis of CH₃OD are shown in Fig. 2. Because the D atom signal is structured, we are able to definitively assign it to the primary photodissociation channel yielding CH₃O+D, as discussed below. The small H atom signal, however, is broad and structureless except for the small number of H atoms that appear at early arrival times (i.e., 18–20 μ s). This part of the spectrum has the same qualitative structure as the D atoms, indicating that this signal derives from isotopic exchange of the chemically labile hydroxyl D in the sample line. Apart from the signal that results from isotopic contamination, the potential sources for the H atom TOF spectrum from CH₃OD include the two primary processes

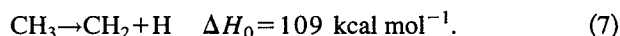
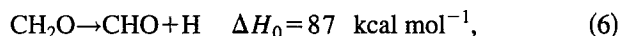
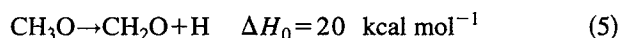




Energy conservation eliminates channel (4) for the portion of the H atom signal arriving before $24.5 \mu\text{s}$ (i.e., this arrival time corresponds to $E_{\text{c.m.}} \sim 24 \text{ kcal mol}^{-1}$ for $\text{CH}_3\text{O} \rightarrow \text{CH}_2\text{O} + \text{H}$). Moreover, the H atom signal does not change markedly in this region, as would be expected if the threshold of an important channel is reached. Furthermore, as discussed below, few if any of the nascent methoxy have sufficient internal energy to decompose to formaldehyde plus hydrogen. From this, we speculate that channel (4) does not contribute appreciably to the H atom signal. The energetic threshold for channel (3) does correspond to the onset of the observed H atom signal. However, as noted above, theoretical studies on this system,^{7,21,22} as well as some of the experiments,^{4,7} indicate that this process is unlikely.

This leads us to consider possible secondary photolysis channels, whereby a photofragment absorbs another photon from the same laser pulse in which it was created. This photoexcited reaction product then fragments further, leading to production of more H atoms. Photolysis fluence dependences were not measured in these experiments. We note that while observation of a nonlinear photolysis fluence dependence can confirm that a process is not a "single photon process," the converse is not true. That is, observation of a linear dependence does not prove that the observed signal arises from a one-photon process.

From what is known about the photochemistry of methanol, the following secondary photolysis channels seem plausible



Nascent photofragments may contain appreciable rovibronic excitation and thus energy from the first photon may appear as translational energy in a secondary photolysis channel. Because of this, any combination of these processes could in principle account for the observed H atom signal. Satyapal *et al.*⁸ also observed D atoms from CD_3OH and found that this signal had a nonlinear photolysis fluence dependence. They tentatively attributed the D atoms to photolysis of CD_3 .

We now turn to the structured part of the spectra. Arrival time spectra of H atom photofragments from CH_3OH photodissociation are shown in Fig. 3. Spectrum (a) was taken with unpolarized 193 nm radiation, while (b) and (c) were obtained with horizontally and vertically polarized radiations, respectively. The spatial arrangement of the molecular beam, polarized photolysis radiation, and the detector is indicated in the inset. We estimate that the polarization ratio achieved with the Brewster plates is $\sim 10:1$, and therefore part of spectrum (c) is due to residual horizontally polarized radiation. This is consistent with the transition dipole moment being perpendicular to the line of departure of the hydrogen that derives from O–H bond rupture. The molecule dissociates on a time scale which is rapid compared to that of

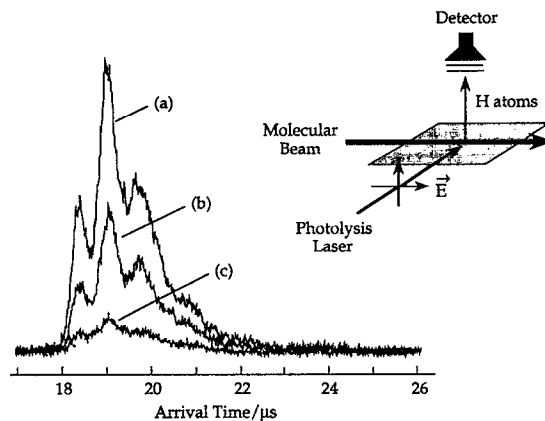


FIG. 3. H atom signal from photolysis of CH_3OH , obtained with flight path of 33.9 cm and (a) unpolarized, (b) horizontally, and (c) vertically polarized 193 nm photolysis radiation. Polarization ratios are estimated at 10:1.

molecular rotation (~ 1 ps). We estimate a spatial anisotropy parameter $\beta \sim -0.7$, in reasonable agreement with Satyapal *et al.*,⁸ who reported $\beta = -0.60 \pm 0.03$.

Translational energy distributions derived from HRTOF spectra of the three methanol isotopomers are shown in Fig. 4; structure is due to methoxy internal excitation. The maximum translational energies are 42.5 ± 1 , 42.5 ± 1 , and $41.2 \pm 1 \text{ kcal mol}^{-1}$ for $\text{CH}_3\text{O} + \text{H}$, $\text{CD}_3\text{O} + \text{H}$, and $\text{CH}_3\text{O} + \text{D}$, respectively. Figure 4 displays probability density versus the quantity $(1 + m_{\text{H}}/m_{\text{CH}_3\text{O}})E_{\text{H}}$ where E_{H} is the lab frame hydrogen translational energy (deuterium replaces hydrogen where appropriate). Values for c.m. translational energies are obtained by adding to this the quantity $(m_{\text{H}}/m_{\text{CH}_3\text{O}})E_{\text{parent}}$, where

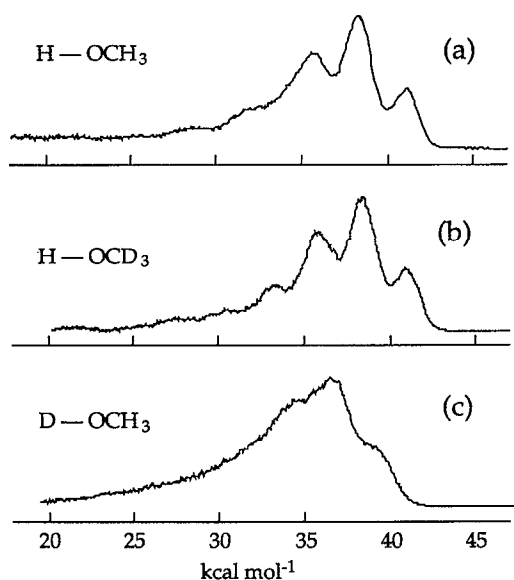


FIG. 4. Translational energy release spectra as determined from the HRTOF spectra: (a) H atoms from CH_3OH ; (b) H atoms from CD_3OH ; and (c) D atoms from CH_3OD . The horizontal axis is $(1 + m_{\text{H}}/m_{\text{CH}_3\text{O}})E_{\text{H}}$, where E_{H} is the laboratory hydrogen translational energy; deuterium replaces hydrogen where appropriate.

E_{parent} is in the lab frame; again, deuterium replaces hydrogen where appropriate. This term accounts for the velocity of the molecular beam. The resulting c.m. values are 42.9 ± 1 , 42.9 ± 1 , and 42.0 ± 1 kcal mol⁻¹ for CH₃O+H, CD₃O+H, and CH₃O+D, respectively.

If these maximum translational energies correspond to ground state methoxy, the corresponding bond dissociation energies can be determined. With this assumption, our results yield bond dissociation energies for CH₃O–H, CD₃O–H, and CH₃O–D of 105 ± 1 , 105 ± 1 , and 106 ± 1 kcal mol⁻¹, respectively, in accord with recent measurements and calculations.^{9–11} The larger CH₃O–D bond energy is due to the change in zero-point energies upon deuteration.^{30,31}

The data presented in Fig. 4 show that translation accounts for a large fraction of the available energy. This is in agreement with the results of Satyapal *et al.*, who reported that the average c.m. translational energy in this channel is 82% of the available energy. However, our results reveal information on how the CH₃O internal energy is distributed.

The spectra in Figs. 4(a) and 4(b) evince a progression, with the first three maxima spaced by 950 ± 100 cm⁻¹. We assign this to the methoxy ν_3 O–CH₃ stretch based on the following: (i) literature values for ν_3 include assignments in fluorescence^{32–34} at 1045 ± 10 cm⁻¹ and a calculated value³⁵ of 1064 cm⁻¹; (ii) the spacing of the observed progression is changed very little by deuteration of the methyl group, ruling out significant methyl hydrogen motion; and (iii) previous studies indicate that initial excitation is localized on the oxygen and dissociation proceeds rapidly on an excited PES. We note that the $S_1 \leftarrow S_0$ photophysics of methanol is reminiscent of the first absorption band of CH₃SH, studied previously in our laboratory.²⁶ In both cases, dissociation of the X–H (X=O,S) bond occurs on a time scale ≤ 1 ps. However, methoxy O–CH₃ stretch excitation following 193 nm photolysis is more extensive than thiomethoxy S–CH₃ stretch excitation following 248 nm photolysis of methyl mercaptan.

The O–CH₃ vibrational progression seen in Figs. 4(a) and 4(b) is also apparent in the photodissociation of CH₃OD, as shown in Fig. 4(c), but the peaks are more poorly resolved. This is attributable to the greater impulsive force imparted to the methoxy by a recoiling deuterium as compared to hydrogen. An estimate of the rotational excitation caused by the departing atom can be made by using the “impulsive model.”³⁶ Briefly, the CH₃ moiety is taken as a structureless particle and the Me–O–H bond angle, α_0 , is assigned the ground state equilibrium value of 108° .³⁷ This yields

$$\frac{E_{\text{rot}}}{E_{\text{avail}}} = \frac{M_{\text{H}}M_{\text{CH}_3} \sin^2 \alpha_0}{(M_{\text{H}} + M_{\text{O}})(M_{\text{CH}_3} + M_{\text{O}}) - M_{\text{H}}M_{\text{CH}_3} \cos^2 \alpha_0} \quad (8)$$

Equation (8) gives values for $E_{\text{rot}}/E_{\text{avail}}$ of 0.026 and 0.049 for H and D, respectively. Inspection of Figs. 4(a) and 4(b) reveals that the energy spacing from threshold to maximum for the first peak in the progression is roughly 600 cm⁻¹ or 0.04 of the available energy. For the case of CH₃O+D shown in Fig. 4(c), the first peak does not display a distinct maximum, but it appears to be shifted from the origin by ~ 1100 cm⁻¹, or 0.08 of the available energy.

The impulsive model predicts the *relative* increase in rotational excitation upon D/H substitution at the oxygen, but underestimates the amount of rotational excitation. Though choosing $\alpha_0 = 108^\circ$ was arbitrary, setting $\alpha_0 = 90^\circ$ to give the maximum rotational excitation results in only a modest increase in the predicted $E_{\text{rot}}/E_{\text{avail}}$ i.e., from 0.026 to 0.028 and from 0.049 to 0.053 for H and D, respectively. Agreement cannot be obtained by adjusting α_0 .

One explanation for the underestimate of methoxy rotational excitation is that torques deriving from the angular part of the excited PES are neglected. This is a known limitation of the impulsive model. Such torque can either decrease or increase product rotation, as has been demonstrated for the cases of ClNO and ClCN, respectively.³⁶ Thus the $1^1A''$ PES may exert torque that increases methoxy rotation.

The present experimental resolution of ~ 170 cm⁻¹ is too low to provide detailed information about methoxy rotational distributions. Furthermore, we cannot rule out the possibility that unresolved features buried within the O–CH₃ progression conceal additional vibrational excitation in modes other than ν_3 . However, if we concern ourselves only with this vibration, the extent of ν_3 excitation in nascent methoxy can be estimated by simulating the data presented in Fig. 4. Specifically, the following expression was used to represent the translational energy distributions of each ν_3 level

$$P(E) = P_{\nu} N_{\nu} (E - E_{\nu})^3 \exp\{-\gamma_{\nu} (E - E_{\nu})\}, \quad (9)$$

where $N_{\nu} = 6\gamma_{\nu}^{-4}$ is a normalization factor and γ_{ν} is an adjustable parameter that varies little from one vibrational level to another. It was found empirically that the γ_{ν} values for entries (a) and (b) are essentially the same for all ν (i.e., $\gamma_{\nu} = 1/200$ cm⁻¹), while the γ_{ν} values for entry (c) are the same for all ν , but are smaller than those for (a) and (b) by a factor of 2/3 (i.e., $\gamma_{\nu} = 1/300$ cm⁻¹). We attach no special significance to Eq. (9). It fits the data (see Fig. 5) and may reflect the CH₃O rotational distribution. However, it does not provide a unique fit.

The P_{ν} values obtained from the fits shown in Fig. 5 are presented in Table II. Despite the latitude in deriving P_{ν} values, the following features are robust: (i) the O–CH₃ stretch vibration is inverted, with $\nu = 1$ having the largest population and measurable population to at least $\nu = 4$; (ii) the average CH₃O vibrational energy is approximately 1700 cm⁻¹, independent of isotopic substitution. This amount of vibrational excitation is considerably greater than that seen following excitation of CH₃SH in its first absorption band at 248 nm. In that case, the thiomethoxy internal energy distribution peaked at $\nu = 0$.²⁶

We also note that at $\nu = 3$, the CD₃O+H spectrum appears more distinct than that of CH₃O+H. This was fit in the simulation with a somewhat broader rotational distribution. Alternate explanations include slight excitation in modes other than ν_3 , e.g., CH stretch, umbrella, and bend modes. Some excitation in these modes is expected, since the C–H bonds are longer and H–C–O bond angle is larger in methoxy than in methanol.^{37,38}

As discussed in the Introduction, the methoxy state distributions reflect forces in photoexcited methanol as it

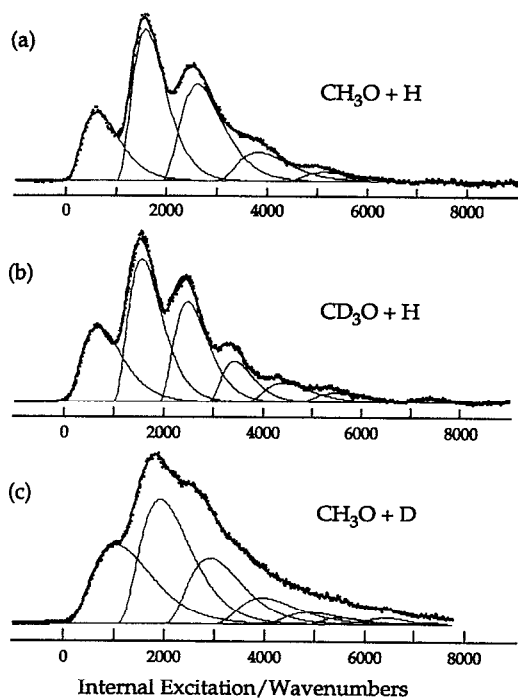


FIG. 5. Internal energy distributions inferred from the translational energy release spectra in Fig. 4, along with simulations, assuming contours as discussed in the text.

evolves on the excited PES. From our data, the dominance of the O–CH₃ stretch progression suggests that this system may be modeled as pseudotriatomic, with CH₃ treated as structureless. This is the approach employed by Marston *et al.* in their theoretical study of methanol photofragmentation.²³

Our translational energy release spectrum resembles the one-dimensional Franck–Condon progression often observed in electronic transitions. This suggests that such a model might provide insight.²⁶ Briefly, ground state MeOH is promoted to the excited PES, where it evolves. In addition to the repulsive force that breaks the O–H bond, the excited PES exerts forces that change the bond distances and angles in the newly forming methoxy. Projecting the excited PES wave function onto a methoxy basis subsumes all fragmentation

TABLE II. Normalized vibrational population distributions for ν_3 O–CH₃ stretch in methoxy from photodissociation of three isotopomers of methanol. Average vibrational energies $\langle f_v \rangle$ were calculated assuming $\nu_3 = 1050 \text{ cm}^{-1}$, while average rotational energies $\langle f_r \rangle$ were obtained from contour fits.

ν_3 level	P_v for CH ₃ O+H	P_v for CD ₃ O+H	P_v for CH ₃ O+D
$v=0$	0.19	0.21	0.29
$v=1$	0.34	0.30	0.37
$v=2$	0.28	0.23	0.19
$v=3$	0.13	0.11	0.13
$v=4$	0.06	0.09	0.08
$v=5$	---	0.06	---
$\langle f_v \rangle$	0.11	0.12	0.11
$\langle f_r \rangle$	0.05	0.05	0.08

dynamics into a sudden approximation. The width and central position of the excited state wave function were varied to fit the observed progression. Methoxy stretch was modeled as a harmonic oscillator with $\nu = 1050 \text{ cm}^{-1}$,^{33,35} and $R_{\text{eq}} = 1.39 \text{ \AA}$.³⁸ Note that the change in C–O bond length between the electronic ground states of methanol and methoxy is only 0.03 \AA ,³⁸ which is too small to account for the observed progression. The best fit was $\nu_3 \sim 1000 \text{ cm}^{-1}$ and $R_{\text{eq}} = 1.52 \text{ \AA}$, suggesting weakening of the C–O bond on the excited PES.

A more thorough approach to computational modeling of the excited state dynamics in this multidimensional system was presented by Marston *et al.*²³ By treating CH₃ as a structureless particle and holding the Me–O–H angle fixed, wave packet propagation on their calculated excited surface was used to examine the dynamics of competitive $R_{\text{O-H}}$ vs $R_{\text{C-O}}$ bond rupture. In their studies, the Franck–Condon region accessed the excited PES in a region that enabled the C–O stretch vibration to evolve adiabatically from the ground state to products. This is not what happens. There is significant CH₃O vibrational excitation. The difference can probably be reconciled by shifting the Franck–Condon region to a different part of the excited PES and/or by changing the shape of the surface, especially near the ridge that separates the two product channels. Such changes, which lead to O–CH₃ excitation, may also account for the small amount of CH₃+OH product inferred by Satyapal *et al.*,⁸ which was not reproduced in the Marston *et al.* calculations.

CONCLUSIONS

Vibrationally resolved c.m. translational energy distributions for the dominant photofragmentation channel of methanol, $\text{CH}_3\text{OH} + h\nu \rightarrow \text{CH}_3\text{O} + \text{H}$, were recorded by using the HRTOF method. Though most of the available energy appears as c.m. translation, a methoxy O–CH₃ stretch progression is observed which is peaked at $v = 1$. This is consistent with a significant change in this coordinate on the excited PES, relative to either ground state methanol or methoxy. Studies with the isotopic variants CD₃OH and CH₃OD reveal that photofragmentation of the latter yields significantly broader features. The extent of this broadening can be rationalized by consideration of the greater exit channel impulse imparted by D relative to H. The impulsive model somewhat underestimates the magnitude of methoxy rotation, as inferred from the rotational contour, suggesting that a torque is exerted by the angular part of the excited PES. H atoms observed from CH₃OD may be attributable to a multiphoton process, such as secondary photolysis of a primary photoproduct.

¹Chem. Eng. News, 17(26), 41 (1993).

²R. Schmiedl, U. Meier, and K. H. Welge, Chem. Phys. Lett. **81**, 495 (1981).

³For a review of early work, see C. Von Sonntag and H.-P. Schuchmann, Adv. Photochem. **10**, 59 (1977).

⁴R. P. Porter and W. A. Noyes, Jr., J. Am. Chem. Soc. **81**, 2307 (1959).

⁵J. Hagege, P. C. Roberge, and C. Vermeil, Ber. Bunsenges. Phys. Chem. **72**, 138 (1968).

⁶O. S. Herasymowich and A. R. Knight, Can. J. Chem. **51**, 147 (1973).

⁷R. J. Buenker, G. Olbrich, H.-P. Schuchmann, B. L. Schurmann, and C. von Sonntag, J. Am. Chem. Soc. **106**, 4362 (1984).

- ⁸S. Satyapal, J. Park, R. Bersohn, and B. Katz, *J. Chem. Phys.* **91**, 6873 (1989).
- ⁹*J. Phys. Chem. Ref. Data* **11**, Suppl. 2 (1982).
- ¹⁰L. Batt and R. D. McCulloch, *Int. J. Chem. Kinet.* **8**, 491 (1976).
- ¹¹L.A. Curtiss and D. A. Pople, *J. Chem. Phys.* **95**, 4040 (1991).
- ¹²C. W. Bauschlicher, Jr., S. R. Langhoff, and S. P. Walch, *J. Chem. Phys.* **96**, 450 (1992).
- ¹³D. C. McKean, J. L. Duncan, and L. Batt, *Spectrochim. Acta A* **29**, 1037 (1973).
- ¹⁴D. D. Wagman, W. H. Evans, V. B. Parker, S. H. Schumm, I. Halow, S. M. Bailey, K. L. Churney, and R. L. Nutall, *J. Phys. Chem. Ref. Data* **11**, Suppl. 1 (1982).
- ¹⁵For a thorough review of the experimental literature on the thermochemistry of neutral and cationic CH₃O and CH₂OH, see B. Ruscic and J. Berkowitz, *J. Chem. Phys.* **95**, 4033 (1991).
- ¹⁶D. R. Salahub and C. Sandorfy, *Chem. Phys. Lett.* **8**, 71 (1971).
- ¹⁷J. G. Calvert and J. N. Pitts, Jr., *Photochemistry* (Wiley, New York, 1966).
- ¹⁸H. Tsumbomura, K. Kimura, K. Kaya, J. Tanaka, and S. Nagakura, *Bull. Chem. Soc. Jpn.* **37**, 417 (1964).
- ¹⁹(a) M. B. Robin and N. A. Kuebler, *J. Electron. Spectrosc.* **1**, 13 (1972); (b) M. B. Robin, *Higher Excited States of Polyatomic Molecules* (Academic, New York, 1974), Vol. 1.
- ²⁰W. R. Wadt and W. A. Goddard III, *Chem. Phys.* **18**, 1 (1976).
- ²¹E. Kassab, J. T. Gleghorn, and E. M. Evleth, *J. Am. Chem. Soc.* **105**, 1746 (1983).
- ²²C. Larrieu, A. Dargelos, M. Chaillet, and B. Monfilih, *Nouv. J. Chim.* **5**, 365 (1981).
- ²³C. C. Marston, K. Weide, R. Schinke, and H. U. Suter, *J. Chem. Phys.* **98**, 4718 (1993).
- ²⁴L. Schneider, W. Meier, K. H. Welge, M. N. R. Ashfold, and C. Western, *J. Chem. Phys.* **92**, 7027 (1990).
- ²⁵M. N. R. Ashfold, I. R. Lambert, D. H. Mordaunt, G. P. Morely, and C. Western, *J. Phys. Chem.* **96**, 2938 (1992).
- ²⁶J. Segall, Y. Wen, R. Singer, M. Dulligan, and C. Wittig, *J. Chem. Phys.* **99**, 6600 (1993).
- ²⁷J. Segall, Y. Wen, R. Singer, C. Wittig, A. García-Vela, and R. B. Gerber, *Chem. Phys. Lett.* **207**, 504 (1993).
- ²⁸C. Jaques, L. Valachovic, S. Ionov, E. Böhmer, Y. Wen, J. Segall, and C. Wittig, *J. Chem. Faraday Trans.* **89**, 1419 (1993).
- ²⁹H. Zacharias, H. Rottke, J. Danon, and K. H. Welge, *Opt. Commun.* **37**, 15 (1981).
- ³⁰A. Serrallach, R. Meyer, and H. H. Günthard, *J. Mol. Spectrosc.* **52**, 94 (1977).
- ³¹A. J. Barnes and H. E. Hallam, *Trans. Faraday Soc.* **66**, 1920 (1970).
- ³²T. Ebata, H. Yangishita, K. Obi, and I. Tanaka, *Chem. Phys.* **69**, 27 (1982).
- ³³S. D. Brossard, P. G. Carrick, E. L. Chappell, S. L. Hulegaard, and P. C. Engelking, *J. Chem. Phys.* **84**, 2459 (1986).
- ³⁴S. C. Foster, P. Misra, T.-Y. D. Lin, C. P. Damo, C. C. Carter, and T. A. Miller, *J. Phys. Chem.* **92**, 5914 (1988).
- ³⁵S. M. Colwell, R. D. Amos, and N. C. Handy, *Chem. Phys. Lett.* **109**, 524 (1984).
- ³⁶R. Schinke, *Photodissociation Dynamics* (Cambridge University, Cambridge, 1992).
- ³⁷M. C. L. Gerry, R. M. Lees, and G. Winnewisser, *J. Mol. Spectrosc.* **61**, 231 (1976).
- ³⁸T. Momose, Y. Endo, and E. Hirota, *J. Chem. Phys.* **88**, 5338 (1988).